J. Biochem. **133**, 263–270 (2003)
DOI: 10.1093/jb/mvg036

RNA Aptamers Targeted to Domain II of Hepatitis C Virus IRES That Bind to Its Apical Loop Region

Kunio Kikuchi[1,2], Takuya Umehara[1,2], Kotaro Fukuda[1], Joonsung Hwang[1], Atsushi Kuno[2], Tsunemi Hasegawa[2] and Satoshi Nishikawa[*,1]

[1]Institute for Biological Resources and Functions, National Institute of Advanced Industrial Science and Technology (AIST), Tsukuba, Ibaraki 305-8566; [2]Faculty of Science, Yamagata University, Yamagata 990-8560

Received October 26, 2002; accepted November 27, 2002

The internal ribosome entry site (IRES) is important for translation of hepatitis C virus (HCV) mRNA and has a unique RNA structure containing conserved domains I to IV. To investigate the function of domain II, we selected RNA aptamers that bind to domain II of HCV IRES by applying a simple and convenient selection method using a hybridized tag for fixing domain II RNA on magnetic beads instead of synthesizing long RNA. In addition, we employed surface plasmon resonance (SPR) technology to measure the binding affinity of each generation and to obtain detailed kinetic constants. The selected aptamers have a consensus sequence, 5′-UAUGGCU-3′, which is complementary to the apical loop of domain II. The loop–loop interaction between the consensus sequence and domain II was confirmed by mutagenesis and nuclease mapping analyses. Binding affinities were dependent on the local structure containing the conserved sequence. The aptamers could inhibit IRES-dependent translation.

Key words: aptamer, HCV, *in vitro* selection, IRES, loop–loop interaction, RNA structure.

RNA–RNA interactions play important roles in many biological and biotechnological events, such as mRNA–tRNA, ribozyme–substrate RNA, and siRNA-mRNA interactions (*1*). In the replication system of HIV, it is important that the dimerization initiation site (DIS) dimerizes by a loop–loop interaction (kissing interaction) (*2*). For *Col*E1 and related plasmids, loop–loop interactions are involved in the regulation of the plasmid copy number (*3*, *4*). Barley yellow dwarf virus mRNA can cross-talk between its 5′ untranslated region (5′ UTR) and its 3′ UTR by direct RNA-RNA interactions (*5*). Communication of 5′ UTR and 3′ UTR facilitates cap-independent translation (*6*, *7*).

Hepatitis C virus (HCV) is a positive-stranded RNA virus that is the main causative infectious agent of post-transfusion hepatitis. The 9.5-kb RNA genome encodes a precursor polypeptide (*8*), and translation starts within the 5′ untranslated region (5′ UTR) at an internal ribosome entry site (IRES). The IRES is highly conserved among HCV strains and mediates translation initiation of the HCV genome in a 5′ cap-independent manner (*9*). It is known that HCV IRES is bound by the host-cell small ribosomal subunit (40S) and by eukaryotic initiation factor 3 (eIF3), and these interactions allow the start of translation. The IRES RNA has four conserved stem-loop structures (I to IV in Fig. 1A), which have been identified on the basis of thermodynamics, physiology, mutational analysis and nuclease mapping (reviewed in *10*). Recently, the tertiary structure of IRES was determined by cryo-electron microscopy (*11*). Domain IIId and IIIe structures were solved by NMR, and direct interactions between these domains and mammalian 40S ribosomal subunit were demonstrated (*12*). Furthermore, domain IIIabc was shown to be a four-way junction structure by X-ray crystallography (*13*), and IIIb was shown to be an internal loop by NMR (*14*). Both regions are critical for binding to eIF3. Some substitutions in domain III entirely abolish IRES activity (*12*, *15*). Translation starts from the initiator AUG in domain IV. Substitutions that increased the stability of the stem-loop structure in domain IV decreased translation activity (*16*). The structure of this domain is thus important for correct binding of the ribosome at the AUG codon.

While the structure-function relationships of domains III and IV of HCV IRES have been well studied, structural and functional information on domain II is limited. Domain II is essential for HCV IRES dependent translation. The single-stranded region between domain II and domains III-IV is thought to function as a hinge and provide flexibility in both domains. It has been shown that domain II does not directly interact with 40S and eIF3, and that interaction between domain II and the coding region or another site induces a conformational arrangement of coding RNA near the E site (*11*). Indeed, IRES activity is decreased in some mutants (*17*, *18*). A recent NMR study strongly suggests that domain II forms an independent structure and does not interact with other IRES parts (*19*).

In vitro selection, namely, SELEX (systematic evolution of ligands by exponential enrichment), is a useful strategy for isolating nucleic acid sequences that have a high affinity for a target molecule from a randomized oligonucleotide pool (*20*, *21*). As well as producing ligands for protein, organic, dyes and amino acid targets, RNA

[*]To whom correspondence should be addressed. Tel: +81-298-61-6085, Fax: +81-298-61-6159, E-mail: satoshi-nishikawa@aist.go.jp

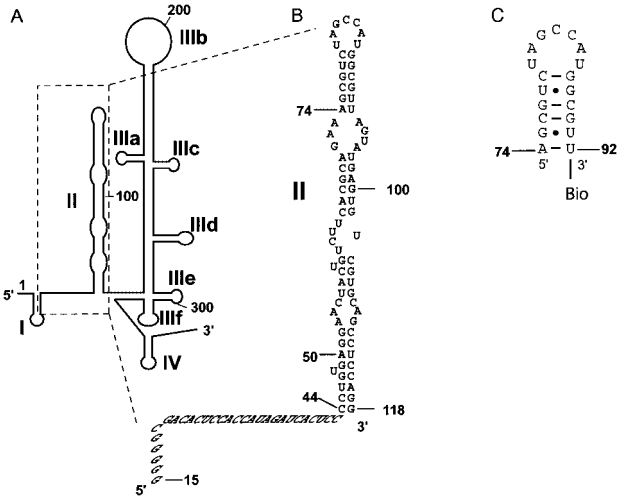

Fig. 1. **HCV IRES RNA.** (A) Schematic structure of the HCV IRES RNA. Structural domains are shown by I to IV. Nucleotide numbers are indicated. (B) Nucleotide sequence of domain II RNA used in this study. Italic letters indicate the sequence that is complementary to biotinylated DNA probe. (C) Nucleotide sequence of the 3′ biotinylated apical region of domain II.

molecules that bind to HIV TAR (*22*), DIS (*23*), and 16S ribosomal RNA (*24*) have been isolated. Recently, Aldaz-Carroll *et al.* selected aptamers against domain IV of HCV IRES. An internal loop of the aptamer interacted with an apical loop of domain IV (*25*). We attempted to obtain RNA aptamers that bind to domain II of HCV IRES to investigate function of domain II, to generate a potential tool for HCV IRES detection, and to develop an inhibitor of translation of HCV mRNA. To screen such aptamers against RNA targets, a convenient selection method was developed using a hybridized tag instead of a synthesized long target RNA molecule. In addition, to screen good aptamers efficiently, we used surface plasmon resonance (SPR) technology. The selected aptamers are expected to provide information on, for example, RNA–RNA interaction between IRES and other cellular RNA. The aptamers inhibiting IRES activity may lead to anti-HCV drugs.

MATERIALS AND METHODS

Oligonucleotides, RNA Pools, and a Target RNA—Template DNAs for RNA pools, primers for PCR, and 3′-biotinylated deoxyoligonucleotides were obtained from Espec Oligo Service. Phosphoramidites for RNA chemical synthesis were purchased from Glen Research. The templates and PCR primers were as follows (T7 promoter region is underlined and N denotes A, G, C, or T): template DNA for N30V pool, 5′-AGTAATACGACTCACTATAGGGAGAATTCCGACCAGAAG-(N30)-CCTTTCCTCTCTCCTTCCTCTTCT-3′; template DNA for N30H pool, 5′-TGTAATACGACTCACTATAGGTAGATACGATGGA-(N30)-CATGACGCGCAGCCA-3′; 5′-end primer for preparation of dsDNA of N30V pool, 5′-AGTAATACGACTCACTATA-3′; 5′-end primer for selection cycles of N30V pool, 5′-AGTAATACGACTCACTATAGGGAGAATTCCGACCAGAAG-3′; 3′-end primer of N30V pool, 5′-AGAAGAGGAAGGAGAGAGGAAAGG-3′; 5′-end primer of N30H pool, 5′-TGTAATACGACTCACTATAGGTAGATACGATGGA-3′; 3′-primer of N30H pool, 5′-TGGCTGCGCGTCATG-3′. 5′-primer for HCV IRES domain II, 5′-TGTAATACGACTCACTATAGGGGGCGACACTCCACCATAGATCACTCC-3′; 3′-primer for domain II, 5′-CCTGGAGGCTGCACGACACTCATACTAA-3′; biotinylated DNA probe, 5′-GGAGTGATCTATGGTGGAGTGTCGCCCCC-3′. The 3′-biotinylated apical region of domain II, 5′-AGCGUCUAGCCAUGGCGUU-Bio-3′, was chemically synthesized using a DNA/RNA synthesizer (model 394; Applied Biosystems). Products were purified as described in the user bulletin ABI (no. 53; 1989).

Two kinds of random-sequenced RNA pools were prepared as follows. Template DNA (N30V: 800 μg, 28 nmol) was converted to double-stranded DNA (dsDNA) by PCR with an equal amount of 3′-end primer (1 μM). The PCR (1 ml × 28 tubes) was carried out for 6 cycles, and dsDNA was recovered by ethanol precipitation. The dsDNA (4 μM) was re-amplified by PCR with 8 μM 5′-end and 3′-end primers. PCR (1 ml × 10 tubes) was carried out for 8 cycles. The re-amplified DNA (~3 mg) was recovered by ethanol precipitation. Using 1.4 mg of the dsDNA, a random RNA pool was generated by *in vitro* transcription (100 μl ×11 tubes) with T7 RNA polymerase (T7 Ampliscribe kit, Epicentre Technology) and purified using a Biospin 30 (BioRad). The final amount of the random RNA pools of N30V was approximately 129 mg. An N30H random RNA pool was prepared similarly. Initial template DNA (900 μg, 24 nmol) was converted to dsDNA. Using 0.25 mg from 1.2 mg of PCR product, the dsDNA was re-amplified. Using 0.65 mg of obtained 1.7 mg re-amplified dsDNA, random RNA was transcribed *in vitro* and purified by polyacrylamide gel electrophoresis (PAGE) containing 7 M urea. The final amount of RNA was approximately 2.2 mg.

HCV IRES domain II RNA (nt number 15–118; Fig. 1) was generated by *in vitro* transcription with T7 RNA polymerase and a PCR fragment from an IRES-encoding vector, p5′IL-U3′X (from Prof. Shimotohno). Purification was carried out as described above.

In Vitro Selection of Aptamers—Biotinylated DNA probe (0.5 μM) was hybridized to domain II of IRES RNA (2 μM) and then mixed with streptavidin magnetic beads (0.1 mg of Streptavidin MagneSphere Paramagnetic Particles, Promega, or 0.4 mg of MAGNOTEX-SA, Takara) in 100 μl of buffer E (20 mM HEPES-KOH, pH 7.9 containing 200 mM KCl and 5 mM $MgCl_2$), and washed with buffer E. Approximately 100 pmol of biotinylated DNA can be bound per bead. Ten nmol of RNA pool was heat-denatured at 94°C for 2 min, cooled to room temperature and pretreated with biotinylated DNA probe immobilized to streptavidin beads for 5 min to remove non-specific binders. Free RNAs were recovered and mixed with probe-IRES immobilized to streptavidin beads. The reaction mixture (500 μl) was incubated for 5 min in buffer E at room temperature. To minimize contamination by non-specific binders, streptavidin beads from different suppliers were alternately used. The IRES RNA-aptamer complexes were magnetically separated and washed with buffer E. The IRES-bound RNAs were eluted at 94°C, recovered by ethanol precipitation, and reversed-transcribed using avian myeloblastosis virus (AMV) reverse transcriptase (MBI) at 42°C for 1 h. IRES RNA was also eluted by this procedure, but the IRES RNA could not be

reverse-transcribed with the specific primers for pools. The dsDNA product was amplified by PCR (Nippon-Gene), transcribed *in vitro* by T7 RNA polymerase (T7 Ampliscribe kit, Epicentre Technology) and purified on 8% PAGE containing 7 M urea. Obtained RNAs (3–4 nmol) were used for the next cycle of the selection. To increase the stringency of selection conditions, the amount of RNA was decreased from 10 nmol in the first generation to 2 nmol in the fourth generation, and the number of washings was increased from one to three.

The PCR product after the fourth selection cycle was introduced into pGEM-T Easy (Promega) and cloned in *Escherichia coli* JM109 strain. Plasmid DNA was isolated from individual clones and sequenced (Big Dye Terminator Sequencing kit, Applied Biosystems) on a 377DNA sequencer. The secondary structure models of selected aptamers were drawn with the MulFold program based on the Zuker algorithm (*26*).

Binding and Kinetic Analyses of Aptamers Using Surface Plasmon Resonance (SPR) Technology—SPR experiments were performed with a BIACORE 2000 apparatus. Biotinylated DNA probe (5 μM) was bound to the surface of a streptavidin-coated sensor chip SA (Biacore) at flow rate of 5 μl/min for 10 min in the buffer E. All procedures were carried out at 20°C. After detection of the binding of probe (usually 1,400 response units; RU), excess unbound probe was washed off with 50 mM NaOH at a flow rate of 10 μl/min for 3 min. Domain II RNA (1 μM; 104 nts in Fig. 1) was immobilized by hybridization with the DNA probe at a flow rate of 2 μl/min for 15 min. Bound domain II was washed twice with 5 μl of 20 mM HEPES-KOH (pH 7.9). RNA samples (125 nM) in buffer E were loaded at a flow rate of 10 μl/min for 2 min for the association phase, and then the dissociation phase was monitored for 3 min. The flow cell containing immobilized probe only was used as a reference.

To assess the complex of aptamer-apical region of domain II, the 3′-biotinylated apical region of domain II was directly bound to the SA chip at flow rate of 10 μl/min in buffer E. For kinetic analysis, about 150 RU of apical region was captured. Aptamer RNAs (12.5–400 nM) were loaded at a flow rate of 10 μl/min for 2 min for the association phase, and then the dissociation phase was monitored for 3 min. In the case of kinetic analysis using full-length domain II, about 700 RU of domain II was captured. The untreated flow cell was used as reference. The collected response data were analyzed with the BIAevaluation program version 3.2. Kinetic parameters were determined by a simple model, A + B = AB. The equations used to describe the reaction model are: $dR/dt = k_{on}C(R_{max} - R) - k_{off}R$, $dR/dt = -k_{off}R$, $dR/dt = -k_{off}R$, where R is the signal response, R_{max} is the maximum response level, C is the molar concentration of the injected sample RNA, and k_{on} and k_{off} are the association rate constant and the dissociation rate constant, respectively.

RNase Mapping of Aptamers and IRES Domain II Complexes—The sample RNAs were labeled at 5′ ends with [γ-^{32}P]ATP by T4 polynucleotide kinase (Takara) and isolated from 8% PAGE containing 7 M urea. Labeled RNAs were denatured at 90°C for 2 min and refolded at room temperature for 15 min. Fifty kcpm of aptamers were partially digested with RNase T_1 (0.05 U, Wako) or RNase A (0.0005 μg, Sigma) in buffer E containing 5 μg of carrier *E. coli* tRNA (Sigma). The reaction was carried out in the presence or absence of IRES domain II (1 μg) and stopped by addition of an equal volume of cold urea dye loading buffer (7 M urea, 0.083% xylencyanol FF, 0.083% bromphenol blue) and by cooling on ice. For the alkaline ladder for markers, aptamers were hydrolyzed with 5 μg carrier tRNA and 6 μl alkaline solution (500 mM $NaHCO_3$ pH 9.25) for 4 min at 90°C, then an equal volume urea dye loading buffer was added. Digested products were subsequently analyzed on 8% PAGE containing 7 M urea.

Inhibition of In Vitro Translation with the Aptamer—Inhibition of *in vitro* translation of luciferase (Luc) mRNA, which coded IRES-Core-Luc-3′ UTR, was performed using rabbit reticulocyte (Flexi Rabbit Reticulocyte Lysates kit, Promega) according to the manufacturer's protocol. Four micrograms of aptamer and 0.5 μg of Luc mRNA, which is transcribed from p5′IL-U3′X, were mixed and incubated for 5 min on ice. Sixteen microliters of reticulocyte lysates was added to the mixtures, and the translation reaction was carried out in the presence of potassium chloride (120 mM) and magnesium acetate (2.5 mM) for 60 min at 30°C. Luciferase activity was measured using the PicaGene kit (Toyo-inki).

RESULTS

Strategy for In Vitro Selection of Aptamers against IRES Domain II Using a Short Tag for Fixing on Beads—We have been interested in locating an accessible binding site of domain II of HCV IRES (Fig. 1A) by RNA aptamers. We developed a simple selection method using a biotinylated DNA probe to fix long target RNA on beads, because such a long sequence usually presents difficulty in chemical synthesis and biotinylation. To solve this problem, domain II (100 nts) was hybridized to biotinylated DNA probe (29 nts), which is complementary to the 5′ extension of domain II, and fixed to streptavidin magnetic beads (Fig. 2A). Ten nmols of RNA pool (G0) was used in the initial selection step. To avoid contamination by non-specific binders, we alternately used streptavidin beads from different suppliers. In addition, RNAs were passed through beads without domain II before every selection cycle, and then mixed with domain II immobilized to streptavidin beads. After washing thoroughly, bound RNAs were eluted and amplified by RT-PCR. For the next cycle of selection, the complementary DNA was transcribed *in vitro* and purified from denaturing PAGE. The recovered RNAs were designated G1. The selection cycle was repeated four times. To select the strongest binders, the stringency of selection was raised by increasing the number of washes from one in the first and second generations to three in the third and fourth. In addition the amount of RNA in the pools was decreased from 10 to 2 nmol from the first to fourth.

Considering the effect of fixed primer sequences for isolating aptamers, we used two kinds of RNA pool with different sequences for primer-binding sites containing a 30 nts random sequence region (Fig. 2B). We were interested to determine whether aptamers converged from different initial pools had the same sequences or not. N30V

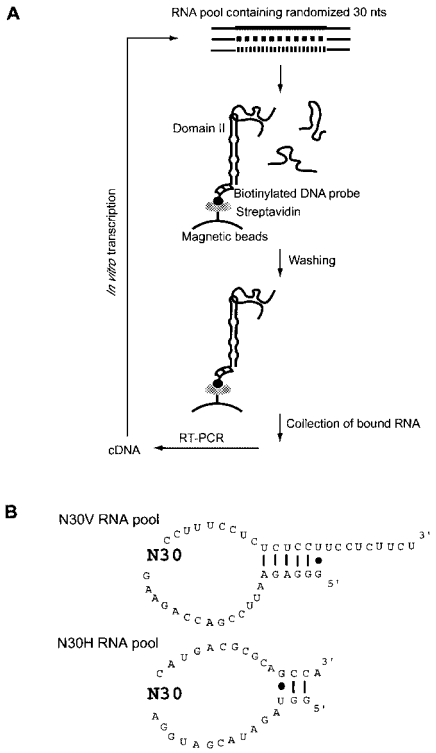

Fig. 2. **(A) Scheme of the *in vitro* selection of RNAs that bind to HCV IRES domain II. (B) Two kinds of initial RNA pool, N30V and N30H, for *in vitro* selection.** Secondary structures are predicted by Mulfold program (*23*). N30 denotes random sequence region.

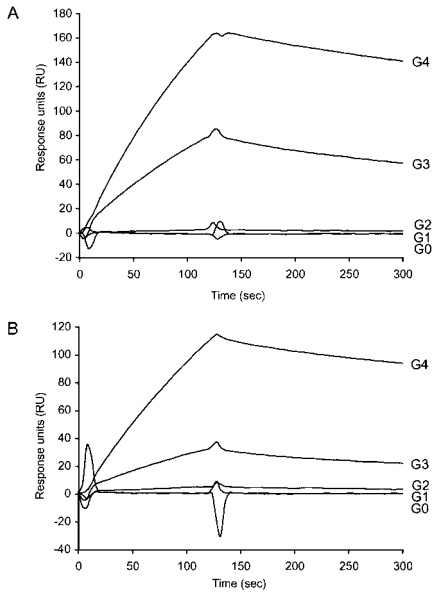

Fig. 3. **Sensorgrams of RNA generations–domain II interaction by BIACORE.** (A) N30V pool. (B) N30H pool. The generations of RNA pools are indicated by G0 to G4. Each RNA pool was applied to BIACORE at a concentration of 125 nM.

pool has a long stem between 5′- and 3′-primers and also 3′-overhang sequences, whereas the N30H pool has a short stem at the ends and only one nucleotide overhang.

Survey of Binding Efficiency Using Surface Plasmon Resonance (SPR) Technology—Increasing of binding affinity at each generation was monitored using the surface plasmon resonance (SPR) technology. This system has been used mainly for protein/protein and protein/small compound interactions and only recently for interactions between nucleic acids (*27–29*). The main feature of this method is that it allows quantitative analysis of binding in real time during selection cycles, in which it is superior to other methods such as gel shift or filter binding assays. Initially, biotinylated DNA probe was immobilized on to a streptavidin sensor (SA) chip, and domain II was fixed to the SA chip through the DNA probe. RNA pools were loaded, binding was monitored, and sensorgrams showing response units (RU) were obtained (Fig. 3). G0 and G1 were not detected from either the N30V or N30H starting pool, but RNA pools from the second generation (G2) showed small responses and those of the third and fourth generations (G3, G4) had larger responses. These sensorgrams showed that RNA evolution occurred as expected in the two pools with different primer sequences in each selection cycle. The dramatic increase of binding from G0 to G4 seems to be due to convergence of sequence.

Sequences and Secondary Structures of G4 RNA Aptamers—To survey what sequences were concentrated during selection, RNA from the fourth generation was cloned, and 34 RNA clones were sequenced (Fig. 4). Almost all RNA clones obtained from the two pools possessed a consensus sequences of seven nucleotides, 5′-UAUGGCU-3′. Fifteen out of 17 clones from the N30V pool and 9 of 17 from the N30H pool contained the consensus sequence. This sequence mainly represents a loop structure in each RNA molecule (Fig. 5), as shown by Mulfold secondary structure prediction. In addition this sequence is complementary to the apical loop of domain II. No other specific structural similarity was found in these RNA molecules. This result indicates that aptamers could interact with the apical loop of domain II of IRES, as in the RNA-RNA kissing interaction (*30*). No effect of difference of primer sequences was observed in aptamer sequences.

Binding Analysis of G4 Aptamers Against the Apical Loop of IRES Domain II—To assess the binding affinity of these G4 aptamers, a 3′ biotinylated 19 nts stem-loop (nt No. 74–92 in Fig. 1C) that corresponds to the apical region of domain II was chemically synthesized and

Table 1. **Rate constants and the dissociation constants of RNA aptamers against the apical stem-loop region of domain II of HCV IRES.**

Aptamer	k_{on} ($\times 10^4$ M^{-1} s^{-1})	k_{off} ($\times 10^{-3}$ s^{-1})	K_D (nM)
1–03	2.5 ± 0.7	0.64 ± 0.03	28 ± 1
1–04	0.55 ± 0.05	2.9 ± 0.1	530 ± 60
1–06	0.02 ± 0.0009	5.9 ± 0.8	33,000 ± 10,000
1–09	2.6 ± 0.6	1.6 ± 0.09	66 ± 2
1–11	1.9 ± 0.4	1.6 ± 0.2	88 ± 2
1–12	0.43 ± 0.1	1.7 ± 0.1	440 ± 100
1–17	4.5 ± 0.4	1.5 ± 0.2	28 ± 1
2–02	2.6 ± 0.7	0.73 ± 0.1	30 ± 0.6
2–03	1.4 ± 0.8	1.1 ± 0.1	47 ± 2
2–12	2.3 ± 0.1	2.2 ± 0.1	93 ± 0.03

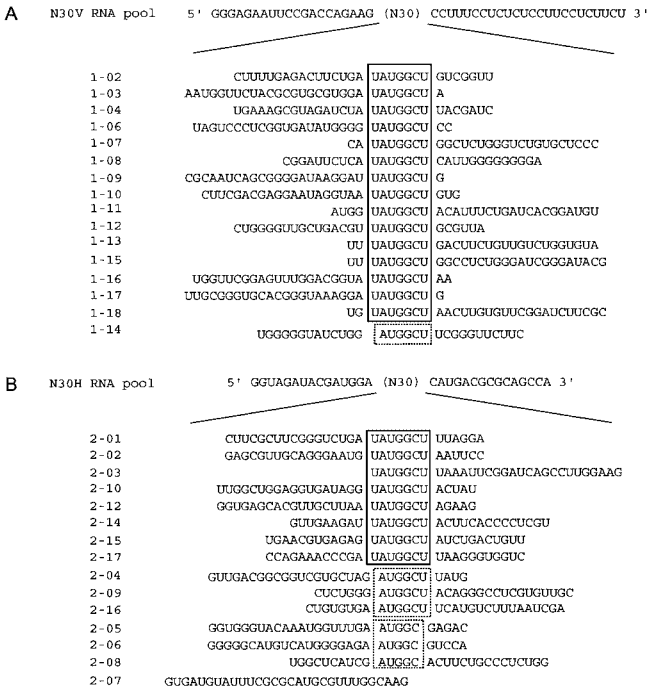

Fig. 4. **Nucleotide sequences of G4 RNA aptamers from N30V RNA pool (A) and N30H pool (B) selected against HCV IRES domain II.** Solid boxed sequence is the conserved sequence. Dotted boxed sequences are semi-conserved sequences.

directly fixed to the streptavidin sensor (SA) chip. Aptamers were loaded at various concentrations from 12.5 to 400 nM. The sensorgrams obtained were analyzed and kinetic constants were calculated with the BIAevaluation program version 3.2 (Table 1). The lowest K_D values (~30 nM) were found for aptamers 1–03, 1–17, and 2–02. These aptamers contains not only a loop structure consisting of the conserved sequence but also two purine bases at both ends of the consensus sequence (Fig. 5). These A-G or A-A pairs seem to be important for stable interaction between aptamers and domain II. In particular, the A-G pair in aptamers 1–17 and 2–02 is observed in other TAR and TAR-aptamer interactions and has been pointed out to be important for stabilization of loop-loop interactions (*22*, *29*, *31*). Aptamers 1–11 and 2–12, in which the conserved sequence is predicted to be located at the stem region, show slightly higher K_D values (~90 nM). The conserved sequence of these aptamers may form a loop structure, as in aptamers 1–17 and 2–02. There seems to be an approximate correlation between binding affinity and models of secondary structure of the conserved sequences, although the predicted model is not always precise.

The K_D values for aptamers 1–04, 1–06, and 1–12 were all 10 to 10^3 times higher than that of the lowest class. Interestingly, the secondary structures of these aptamers show that even the conserved sequence is located in a loop region, but additional Watson-Crick base pairs are possible at both ends of the conserved sequence and more rigid stem structures are suspected in these aptamers (Fig. 5). These rigid stem structures may be unsuitable for stable loop-loop interactions. Aptamers 1–09 and 2–

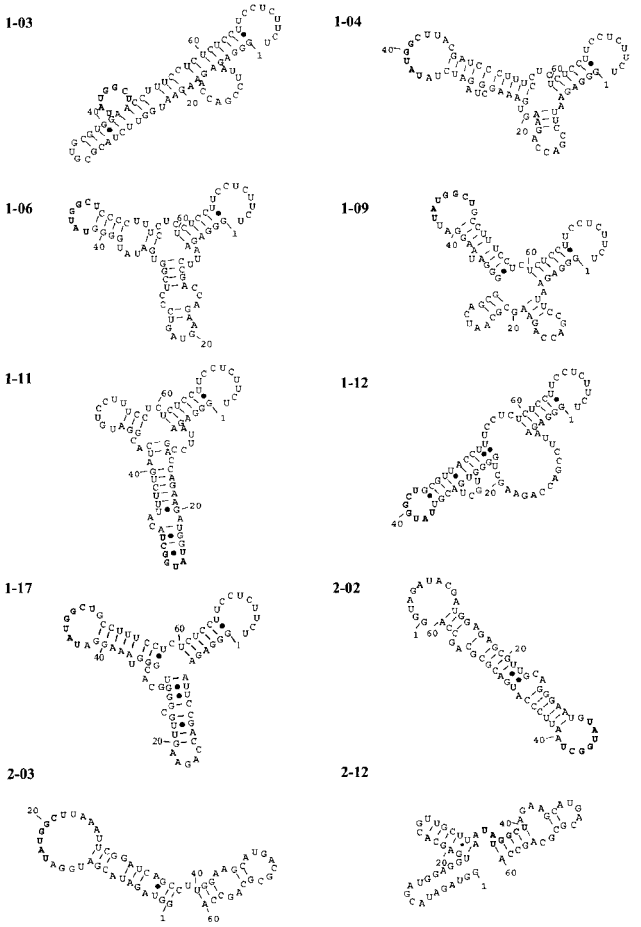

Fig. 5. **RNA secondary structures of G4 RNA aptamers predicted by Mulfold program.** The conserved sequence is shown by bold letters.

03 show intermediate K_D values (40–70 nM), and their structures around the conserved sequence also show an intermediate form, including the possibility of one or more base pairs at ends. The aptamers against HIV TAR and SL1 of HCV 3′ UTR showed the K_D values of 30 and 70 nM, respectively. Corresponding antisense oligomers (6 and 9 nts) showed lower affinity, with binding constants of 5 and 2 μM, respectively (*22*, *25*). Similarly, our aptamers 1–04 and 2–03, which have a more flexible loop than 1–17 and 2–02, had weak affinity. This indicates that structural elements contribute to the affinity of aptamer for the apical region of domain II, in addition to the interaction between the conserved sequences and the apical region of domain II.

We next focused on aptamers 1–17 and 2–02 and analyzed their binding to the natural target sequence, domain II, because these aptamers showed the highest affinity against the short apical loop of domain II but have different secondary structures, namely, 3-way junctions and stem-loop structures, according to secondary structure prediction. The two aptamers were applied to the sensor chip coated in immobilized domain II *via* the biotinylated DNA probe in the same way as in the selection cycles. The binding constant (K_D) of both aptamers was 11 nM, but the kinetic parameters k_{on} and k_{off} were

Table 2. **Rate constants and the dissociation constants of RNA aptamers 1–17 and 2–02 against full-length domain II of HCV IRES.**

Aptamer	k_{on} ($\times 10^4$ M^{-1} s^{-1})	k_{off} ($\times 10^{-3}$ s^{-1})	K_D (nM)
1–17	7.2 ± 1	0.85 ± 0.01	11 ± 0.9
2–02	2.7 ± 0.7	0.29 ± 0.03	11 ± 0.2

different (Table 2). The association (k_{on}) and the dissociation (k_{off}) constants of 1–17 were larger than those of 2–02. The differences of values against the apical region may derive from the differences in the 3-dimensional structures of whole the domain II and the apical region.

We next prepared mutants of 1–17 and 2–02 in which the conserved sequence, 5′-UAUGGCU-3′, was converted to the reverse complementary sequence, 5′-AUACCGA-3′, or the reverse sequence, 5′-UCGGUAU-3′. None of these mutants showed a binding response (data not shown). Accordingly, the conserved UAUGGCU is critical for the interaction between aptamer and domain II. Furthermore, no response was observed when the mutants were applied to the chip with the immobilized biotinylated apical region.

Analysis of Loop–Loop Interaction by Nuclease Mapping—To analyze the correlation of secondary structure with the interaction between aptamers and domain II, RNase probing analysis was applied to aptamers 1–17 and 2–02. RNase T1 (for G) and RNase A (for U and C) digested mainly single-stranded regions, and the patterns were analyzed by denaturing PAGE (Fig. 6, A and B). Clevages occurred mainly in loop regions in both 1–17 and 2–02 aptamers in the absence of domain II, and this result indicates that the predicted secondary structures are correct. Interestingly, cleavage was not detected at the A-G pair at the end of the conserved sequence. This observation supports A-G base-pairing. Next, we analyzed the cleavage pattern in the presence of domain II and found almost the same pattern as that in the absence of domain II, except in the conserved region. The extent of cleavage clearly decreased in this region in both aptamers. This result confirms that the apical loop of domain II and the conserved sequence of aptamers have loop-loop interactions.

Effect of Aptamers on In Vitro Translation Using HCV IRES—Domain II of IRES is important for the translation process of HCV mRNA. It does not interact with other domains of IRES, and the apical loop of domain II seems to make contact with the E-site of the 40S subunit, which is the binding site of deacylated tRNA (*11*). The function of these aptamers was analyzed by an *in vitro* translation assay of IRES-luciferase mRNA. The mRNA contained the 3′ untranslated region (3′ UTR) of the HCV genome after the luciferase gene. The 3′X region in 3′ UTR, conserved among HCV isolates, was suggested to contribute to translation activity, but its detailed function is unknown. IRES-dependent translation was examined in rabbit reticulocyte lysate (RRL) using 0.5 μg of mRNA in the presence of 120 mM potassium chloride and 2.5 mM magnesium acetate, and in the presence or absence of 4 μg of aptamer. In the presence of aptamer 1–17 or 2–02, luciferase activity reduced to 20–40% of the control, but mutant aptamers with changed conserved

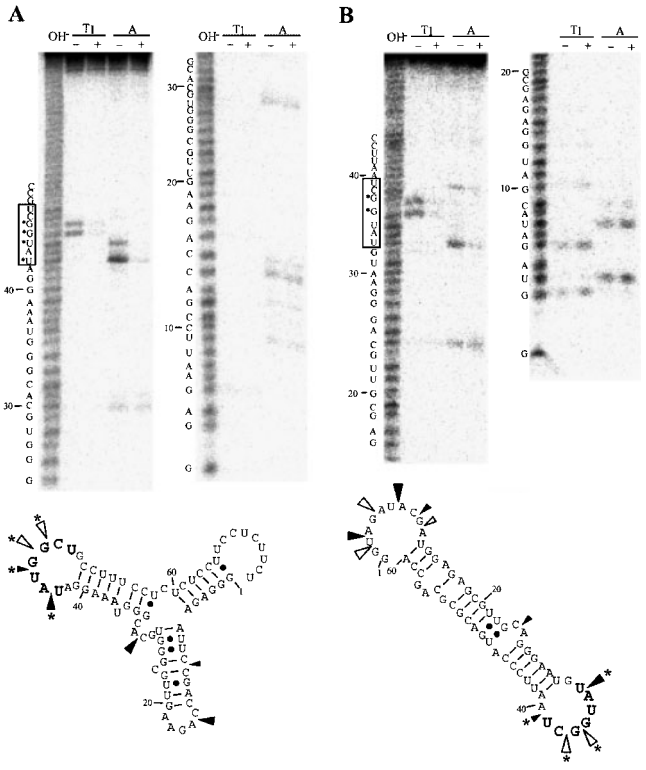

Fig. 6. **RNase mapping analysis of aptamers–IRES domain II interactions.** 5′-End labeled aptamers 1–17 (A) and 2–02 (B) were digested with RNase T_1 or RNase A in the absence (–) or presence (+) of IRES domain II in selection buffer, as indicated at the top of lanes. OH^- shows the alkaline ladder of the aptamer. Secondary structures of aptamers 1–17 and 2–02 were predicted by Mulfold software. Bold letters indicate the consensus region. Open and filled arrowheads indicate sites cleaved by RNase T_1 and RNase A, respectively. Small arrowheads indicate minor cleavage. Asterisks show the positions that were not cleaved by RNases in the presence of IRES-domain II.

loop sequence did not have an inhibitory effect (Fig. 7). This result indicates that the consensus sequence hybridized to the apical loop of domain II of IRES and affected the translation process.

DISCUSSION

The *in vitro* selection method is useful to find a target site of antisense nucleic acids or ribozymes, and actually several short RNA motifs have been used as target molecules (*22–25*). However, this strategy is difficult to apply to long RNA sequences due to synthesis problems. We developed a simple convenient selection system on a solid support via a DNA probe. Our system does not require chemical synthesis of biotinylated long RNA or specific biotinylation of target RNA after transcription *in vitro*. The biotinylated DNA probe is easy to synthesize and inexpensive compared to RNA synthesis, and using the biotinylated DNA probe is applicable for any target RNA molecules.

Selection and analysis of aptamers by gel-shift assay is laborious and time-consuming. We used a surface plasmon resonance (SPR) method for binding analysis between aptamer and domain II of IRES. This chip-based

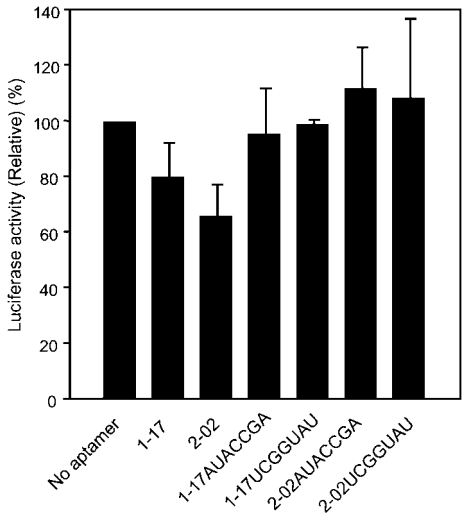

Fig. 7. **Inhibition assay of HCV-IRES dependent *in vitro* translation by RNA aptamers.** Translation activity was measured in terms of luciferase activity, in the absence (No aptamer) or presence of aptamers (1–17, 2–02, and mutant aptamers). In mutants 1–17AUACCGA and 2–02AUACCGA, the conserved sequence 5′-UAUGGCU-3′ was converted to the reverse complementary sequence, 5′-AUACCGA-3′. In mutants 1–17UCGGUAU and 2–02UCGGUAU, the conserved sequence was converted to the reverse sequence.

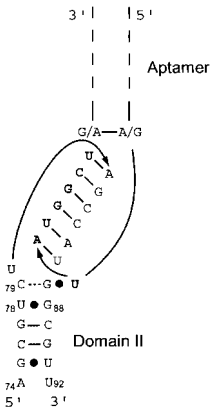

Fig. 8. **Model of loop–loop interaction between the aptamer and the apical region of domain II.** Watson-Crick type base pairs and wobble base pairs are shown by solid lines and filled circles, respectively. The conserved sequence of aptamer is shown by bold letters.

technology is very efficient to monitor molecular interactions in real time with very small amounts of reactants. It allowed us to detect increased binding affinity of RNA pools during selection cycles to analyze binding kinetics of individual aptamers. Kinetic analyses clarified the structure-function relationship of aptamers (Fig. 5 and Table 1) and allowed evaluation of association (k_{on}) and dissociation (k_{off}) constants, which cannot be obtained by usual gel-shift analysis. Aptamers 1–17 and 2–02 had different k_{on} and k_{off} values, even though they had the same K_D value. The difference in affinity among RNA aptamers is mainly dependent on k_{on} values rather than k_{off} values. For example, aptamer 2–02 has a 130-fold larger k_{on} value and 10-fold smaller k_{off} value than 1–06. This system should also allow to fractionation of molecules with higher k_{on} or lower k_{off} values from starting pooled RNAs having the same K_D value. In the case of antisense nucleic acids, a molecule with faster association and slower dissociation is plausible, and our strategy provides a promising means to develop such stable hybrid molecules.

The aptamers targeted to domain II of HCV IRES RNA have the conserved sequence 5′-UAUGGCU-3′, which is complementary to the apical loop of domain II. This conserved sequence is essential for binding of the aptamer, as shown by the results of SPR technology (Table 1) and mutagenesis. The conserved sequence interacts with the apical region of domain II, as shown by RNase mapping (Fig. 6). These results indicate that the apical region of domain II is the most accessible site to exogenous nucleic acids. For RNA loop–loop interactions, all of the nucleotides in each loop are stacked on the 3′-side of the central helix and are involved in pairing interactions (*32*, *33*) (Fig. 8). Interestingly, the 5′-terminal U of the conserved sequence seems to be base-paired with G87 of the stem of domain II, but the base next to the 3′-terminal U is not conserved, even though its counterpart U80 is in the loop region. This is shown by the drastic decrease of cleavage efficiency at the 5′-U of the conserved sequence in the presence of domain II (Fig. 6). U80 is suggested to be important for IRES-dependent translation from the result of mutagenesis (*18*), and this base may be oriented toward the inside of the loop and participate in some interactions.

The aptamers inhibited IRES-dependent translation moderately (Fig. 7). The role of domain II in translation seems to be important, but not as critical as those of other domains such as IIId and IIIe. Accordingly, the inhibitory effect of aptamers might be small. However, aptamers can inhibit translation more strongly by the addition of nucleotide modifications. Indeed, a single 2-thiouridine substitution in the TAR hairpin stabilized TAR–TAR interactions (*34*). It appeared that the function of domain II of HCV IRES is coordination of structural arrangement with domain III-IV of IRES or the coding region. The apical-loop of domain II may function via RNA-RNA or RNA–protein interactions. It was recently shown that domains I and II are necessary for replication (*35*). However, the function of domain II is not yet known. The fact that almost all obtained aptamers are complementary to the apical loop and not other sites of domain II indicates that this apical loop is actually exposed and has some contacts during IRES-dependent translation and also replication. These aptamers are useful for studying these functions of domain II as well as being lead compounds of drugs, sensors or diagnostics of HCV.

We thank Prof. K. Shimotohno (Kyoto University) for providing us the plasmid p5′IL-U3′X. We thank F. Nishikawa for synthesizing biotynylated RNA and helpful discussions. K.K. and K.F. were supported by NEDO fellowships. J.H. was supported by a JSPS fellowship.

REFERENCES

1. Elbashir, S.M., Martinenz, J., Patkaniowska, A., Lendeckel, W., and Tuschl, T. (2001) Functional anatomy of siRNAs for mediating efficient RNA: in *Drosophila melanogaster* embryo lysate. *EMBO J.* **20**, 6877–6888
2. Skripkin, E., Paillart, J.C., Marquet, R., Ehresmann, B., and C., Ehresmann (1994) Idenfication of the primary site of the human immunodeficiency virus type 1 dimerization *in vitro*. *Proc. Natl. Acad. Sci. USA* **91**, 4945–4949
3. Eguchi, Y. and Tomizawa, J-I. (1990) Complex formed by complementary RNA stem-loops and its stabilization by a protein: function of *CoI*E1 Rom protein. *Cell* **60**, 199–209
4. Eguchi, Y., Ito, T., and Tomizawa, J-I. (1991) Antisense RNA. *Annu. Rev. Biochem.* **60**, 631–652
5. Guo, L., Allen, E., and Miller, W.A. (2001) Base-pairing between untranslated regions facilitates translation of uncapped, nonpolyadenylated viral RNA. *Mol. Cell* **7**, 1103–1109
6. Wang, S., Browning, K.S., and Miller, W.A. (1997) A viral sequence in the 3′-untranslated region mimics a 5′ cap in facilitating translation of uncapped mRNA. *EMBO J.* **16**, 4107–4116
7. Wang, S., Guo, L., Allen, E.M., and Miller, W.A. (1999) A potential mechanism for selective control of cap-independent translation by a viral RNA sequence in *cis* and in *trans*. *RNA* **5**, 728–738
8. Kato, N., Hijikata, M., Ootsuyama, Y., Nakagawa, M., Ohkoshi, S., Sugimura, T., and Shimotohno, K. (1990) Molecular cloning of the human hepatitis C virus genome from Japanese patients with non-A, non-B hepatitis. *Proc. Natl. Acad. Sci. USA* **87**, 9524–9528
9. Tsukiyama-Kohara, K., Iizuka, N., Kohara, M., and Nomoto, A. (1992) Internal ribosome entry site within hepatitis C virus RNA. *J. Virol.* **66**, 1476–1483
10. Gallego, J. and Varani, G. (2002) The hepatitis C virus internal ribosome-entry site: a new target for antiviral research. *Biochemical Society Transactions* **30**, 140–145
11. Spahn, C.M.T., Kieft, J.S., Grassucci, R.A., Penczek, P.A., Zhou, K., Doudna, J.A., and Frank, J. (2001) Hepatitis C virus IRES RNA-induced changes in the conformation of the 40S ribosomal subunit. *Science* **291**, 1959–1962
12. Lukavsky, P.J., Otto, G.A., Lancaster, A.M., Sarnow, P., and Puglisi, J.D. (2000) Structures of two RNA domains essential for hepatitis C virus internal ribosome entry site function. *Nat. Struct. Biol.* **7**, 1105–1110
13. Kieft, J.S., Zhou, K., Grech, A., Jubin, R., and Doudna, J.A. (2002) Crystal structure of an RNA tertiary domain essential to HCV IRES-mediated translation initiation. *Nat. Struct. Biol.* **9**, 370–374
14. Collier, A.J., Gallego, J., Klinck, R., Cole, P.T., Harris, S.J., Harrison, G.P., Aboul-ela, F., Varani, G., and Walker, S. (2002) A conserved RNA structure within the HCV IRES eIF3-binding site. *Nat. Struct. Biol.* **9**, 375–380
15. Psaridi, L., Georgopoulou, U., Varaklioti, A., and Mavromara, P. (1999) Mutational analysis of a conserved tetraloop in the 5′ untranslated region of hepatitis C virus identifies a novel RNA element essential for the internal ribosome entry site function. *FEBS Lett.* **453**, 49–53
16. Honda, M., Brown, E.A., and Lemon, S.M. (1996) Stability of a stem-loop involving the initiator AUG controls the efficiency of internal initiation of translation on hepatitis C virus RNA. *RNA* **2**, 955–968
17. Odreman-Macchioli, F., Baralle, F.E., and Buratti, E. (2001) Mutational analysis of the different bulge regions of hepatitis C virus domain II and their influence on internal ribosome entry site translational ability. *J. Biol. Chem.* **276**, 41648–41655
18. Kalliampakou, K.I., Psaridi-Linardaki, L., and Mavromara, P. (2002) Mutational analysis of the apical region of domain II of the HCV IRES. *FEBS Lett.* **511**, 79–84
19. Kim, I., Lukavsky, P.J., and Puglisi, J.D. (2002) NMR study of 100 kDa HCV IRES RNA using segmental isotope labeling. *J. Am. Chem. Soc.* **124**, 9338–9339
20. Tuerk, C. and Gold, L. (1990) Systematic evolution of ligands by exponential enrichment: RNA ligands to bacteriophage T4 DNA polymerase. *Science* **249**, 505–510
21. Ellington, A.D. and Szostak, J.W. (1990) *In vitro* selection of RNA molecules that bind specific ligands. *Nature* **346**, 818–822
22. Duconge, F. and Toulme, J.-J. (1999) *In vitro* selection identifies key determinants for loop-loop interactions: RNA aptamers selective for the TAR RNA element of HIV-1. *RNA* **5**, 1605–1614
23. Lodmell, J.S., Ehresmann, C., Ehresmann, B., and Marquet, R. (2000) Convergence of natural and artificial evolution on an RNA loop-loop interaction: the HIV-1 dimerization initiation site. *RNA* **6**, 1267–1276
24. Tok, J.B.-H., Cho, J., and Rando, R.R. (2000) RNA aptamers that specifically bind to a 16S ribosomal RNA decoding region construct. *Nucleic Acids Res.* **28**, 2902–2910
25. Aldaz-Carroll, L., Tallet, B., Dausse, E., Yurchenko, L., and Toulme, J.-J. (2002) Apical loop-internal loop interactions: a new RNA-RNA recognition motif indentified through in vitro selection against RNA hairpin of the hepatitis C virus mRNA. *Biochemistry* **41**, 5883–5893
26. Zuker, M. (1989) Computer prediction of RNA structure. *Methods Enzymol.* **180**, 202–287
27. Jensen, K.K., Orum, H., Nielsen, P.E., and Norden, B. (1997) Kinetics for hybridization of peptide nucleic acids (PNA) with DNA and RNA studied with the BIAcore technique. *Biochemistry* **36**, 5072–5077
28. Nakatani, K., Sando, S., and Saito, I. (2001) Scanning of guanine-guanine mismatches in DNA by synthetic ligands using surface plasmon resonance. *Nat. Biotechnol.* **19**, 51–55
29. Duconge, F., Di Primo, C., and Toulme, J.-J. (2000) Is a closing "GA pair" a rule for stable loop-loop RNA complexes? *J. Biol. Chem.* **275**, 21287–21294
30. Wagner, E.G. and Simons, R.W. (1994) Antisense RNA control in bacteria, phage, and plasmids. *Annu. Rev. Microbiol.* **48**, 713–742
31. Darfeuille, F., Arzumanov, A., Gryaznov, S., Gait, M.J., Di Primo, C., and Toulme, J.-J. (2002) Loop-loop interaction of HIV-1 TAR RNA with N3′->P5′ deoxyphosphoramidate aptamers inhibits *in vitro* Tat-mediated transcription. *Proc. Natl. Acad. Sci. USA* **99**, 9709–9714
32. Chang, K.-Y. and Tinoco, I.Jr (1997) The structure of an RNA "kissing" hairpin complex of the HIV TAR hairpin loop and its complement. *J. Mol. Biol.* **269**, 52–66
33. Batey, R.T., Rambo, R.P., and Doudna, J.A. (1999) Tertiary motifs in RNA structure and folding. *Angew. Chem. Int. Ed.* **38**, 2326–2343
34. Nair, T.M., Myszka, D.G., and Davis, D.R. (2000) Surface plasmon resonance kinetic studies of the HIV TAR RNA kissing hairpin complex and its stabilization by 2-thiouridine modification. *Nucleic Acids Res.* **28**, 1935–1940
35. Friebe, P., Lohmann, V., Krieger, N., and Bartenschlager, R. (2001) Sequences in the 5′ nontranslated region of hepatitis C virus required for RNA replication. *J. Virol.* **75**, 12047–12057